

Supporting Information:

## **A highly efficient photoelectrochemical sensor for detection of chlorpyrifos based on 2D/2D $\beta$ -Bi<sub>2</sub>O<sub>3</sub>/g-C<sub>3</sub>N<sub>4</sub> heterojunctions**

Haixia Wang<sup>a,b</sup>, Dong Liang<sup>a</sup>, Yan Xu<sup>a</sup>, Xiang Liang<sup>a</sup>, Xiaoqing Qiu<sup>\*a,b</sup> and Zhang Lin<sup>\*c</sup>

### **Contents**

#### **Figures**

**Fig.S1.** XRD pattern of the product without the addition of I<sup>-</sup> ions.

**Fig.S2.** FT-IR spectra of CNNs.

**Fig.S3.** SEM images of CNNs (A),  $\beta$ -Bi<sub>2</sub>O<sub>3</sub> (B) and TEM images of  $\beta$ -Bi<sub>2</sub>O<sub>3</sub>/CNNs 2% (C). Elemental EDX mapping images of  $\beta$ -Bi<sub>2</sub>O<sub>3</sub>/CNNs composites (D-H).

**Fig. S4.** The wide scan XPS survey spectra of CNNs,  $\beta$ -Bi<sub>2</sub>O<sub>3</sub>,  $\beta$ -Bi<sub>2</sub>O<sub>3</sub>/CNNs 2%.

**Fig. S5** UV-vis absorption spectra of CNNs obtained after hydrothermal treatment with different concentrations of NaOH.

**Fig. S6.** The intensity spectrum of visible light.

**Fig. S7.** Chemical structural formulas of Chlorpyrifos, parathion-methyl, imidacloprid and acetamiprid.

#### **Tables**

**Table S1.** Energy band levels of  $\beta$ -Bi<sub>2</sub>O<sub>3</sub> and CNNs (E vs. NHE).

**Table S2.** Calculation of the absorbed photo numbers in each semiconductor.

**Table S3.** Comparison of analytical parameters for chlorpyrifos detection in literatures.

**Table S4.** The relative standard deviation of three  $\beta$ -Bi<sub>2</sub>O<sub>3</sub>-/CNNs 2%-based photoelectrode

**Table S5.** Determination results of Chlorpyrifos in real sample by the PEC method (n = 3).

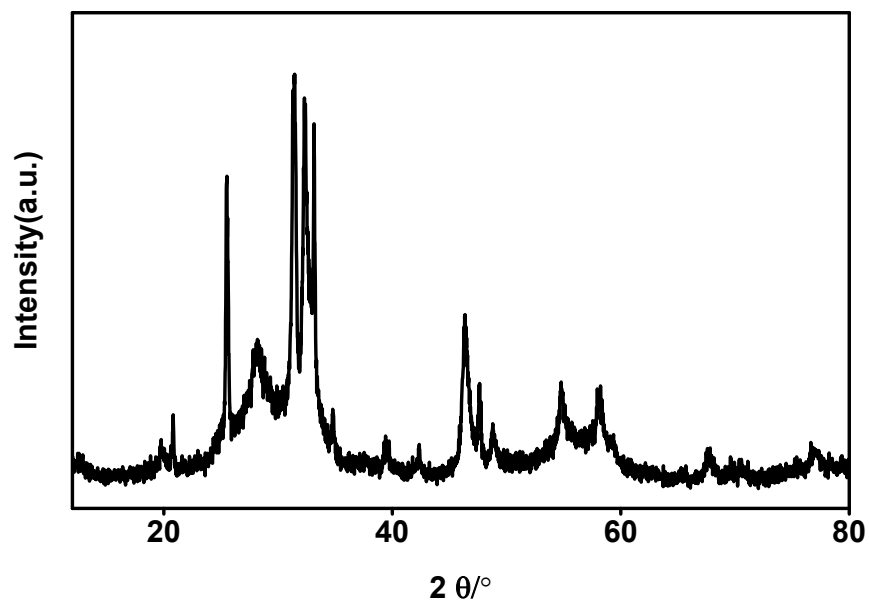


**Fig.S1** XRD pattern of the product without the addition of I<sup>-</sup> ions.

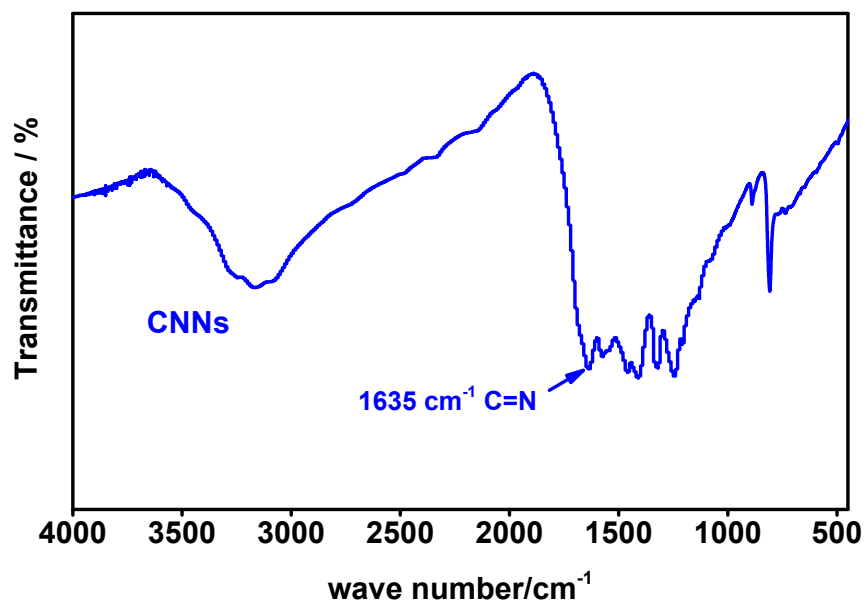


**Fig.S2** FT-IR spectra of CNNs.

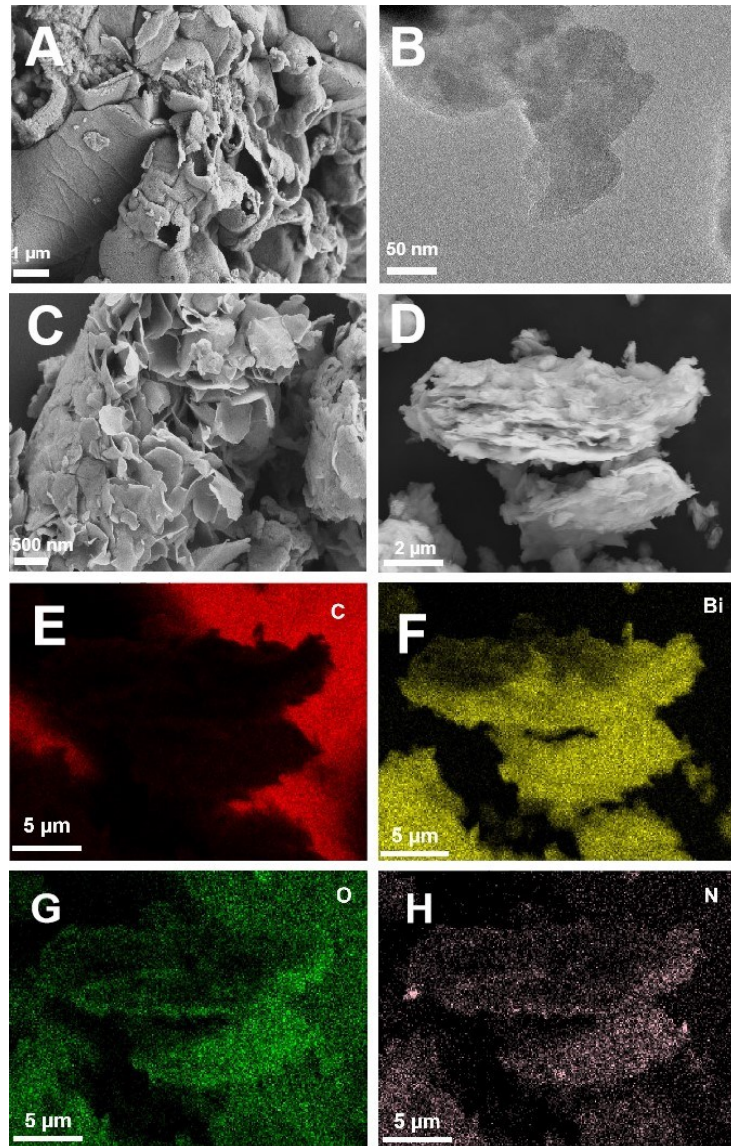


**Fig.S3** SEM images of CNNs (A),  $\beta$ -Bi<sub>2</sub>O<sub>3</sub> (C) and TEM images of CNNs 2% (B). Elemental EDX mapping images of  $\beta$ -Bi<sub>2</sub>O<sub>3</sub>/CNNs composites (D-H).

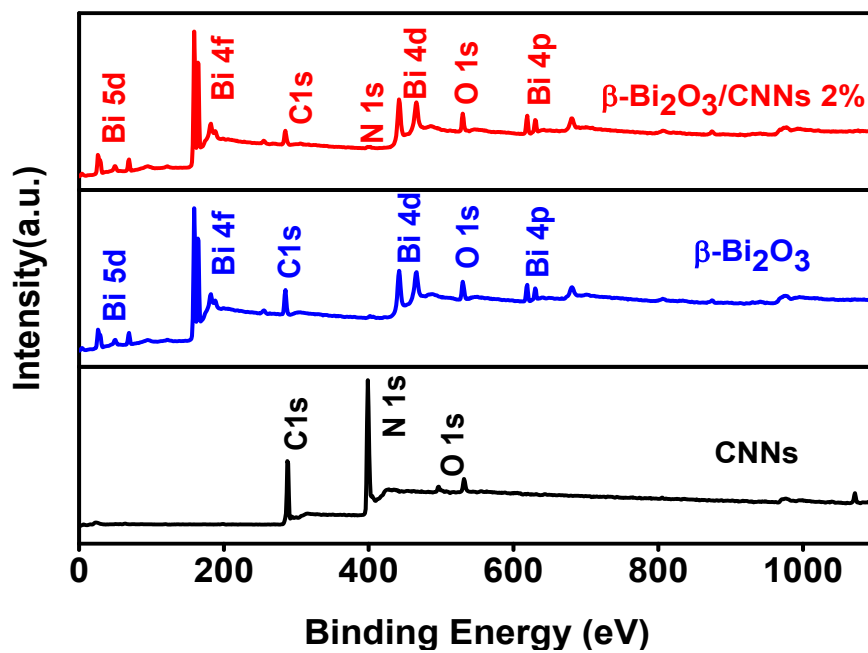


Fig. S4 The wide scan XPS survey spectra of CNNs ,  $\beta\text{-Bi}_2\text{O}_3$  ,  $\beta\text{-Bi}_2\text{O}_3/\text{CNNs}$  2%.

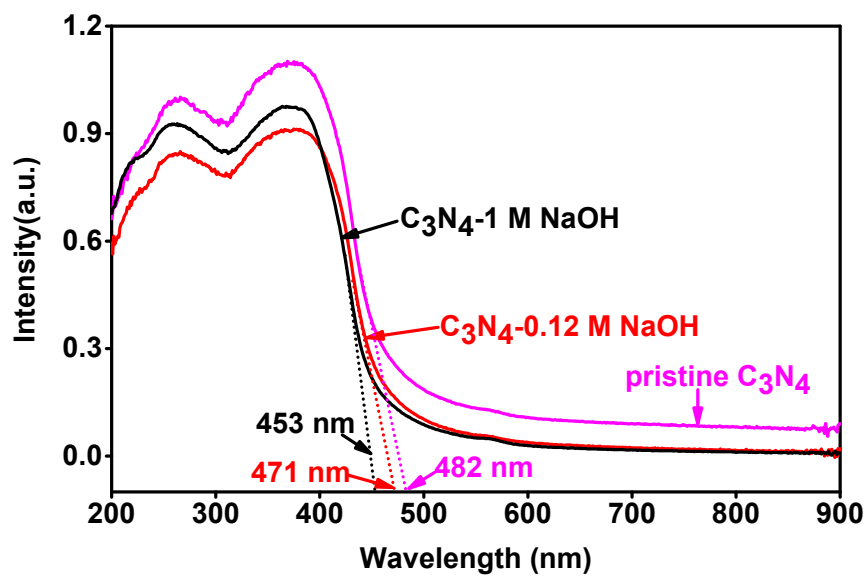
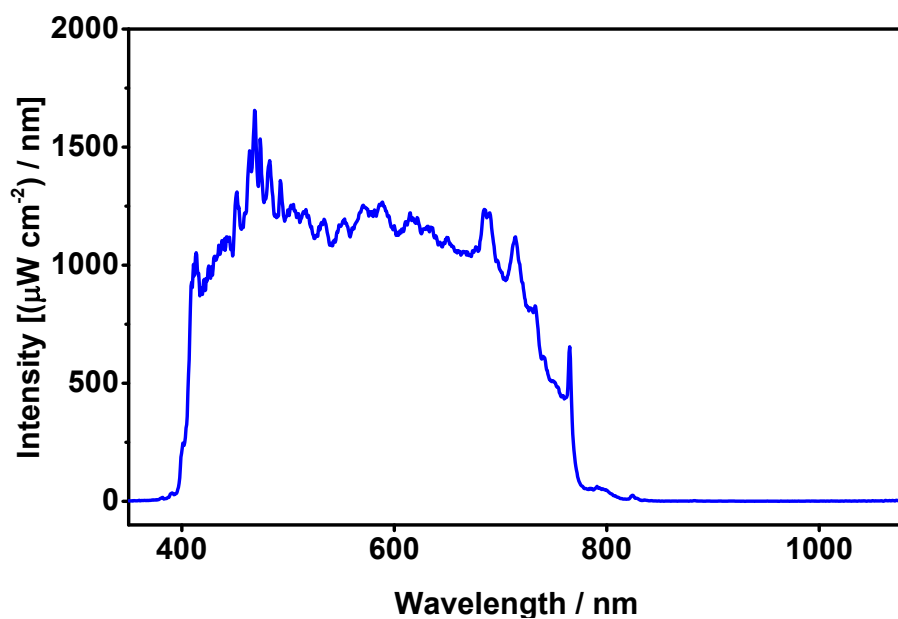
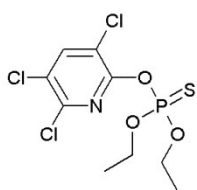


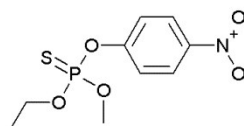
Fig. S5 UV-vis absorption spectra of CNNs obtained after hydrothermal treatment with different concentrations of NaOH.



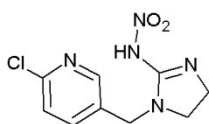
**Fig. S6** The intensity spectrum of visible light.



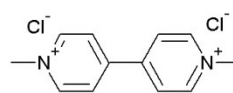
Chlorpyrifos



Parathion methyl



Imidacloprid



Methyl viologen

**Fig. S7** Chemical structural formulas of Chlorpyrifos, parathion-methyl, imidacloprid and acetamiprid.

**Table S1.** Energy band levels of  $\beta$ -Bi<sub>2</sub>O<sub>3</sub> and CNNs (E vs. NHE).

<b>Samples</b>	<b>E<sub>g</sub> (eV)</b>	<b>E<sub>CB</sub> (eV)</b>	<b>E<sub>VB</sub> (eV)</b>
<b><math>\beta</math>-Bi<sub>2</sub>O<sub>3</sub></b>	<b>2.19</b>	<b>0.827</b>	<b>3.017</b>
<b>CNNs</b>	<b>2.51</b>	<b>-1.093</b>	<b>1.417</b>

**Table S2.** Calculation of the absorbed photo numbers in each semiconductor.

<b>sample</b>	<b>CNNs</b>	<b><math>\beta</math>-Bi<sub>2</sub>O<sub>3</sub></b>	<b><math>\beta</math>-Bi<sub>2</sub>O<sub>3</sub>/CNNs 2%</b>
<b>absorbed photon number</b>	<b><math>2.68 \times 10^{14}</math></b>	<b><math>1.70 \times 10^{16}</math></b>	<b><math>1.71 \times 10^{16}</math></b>
<b>R<sup>a</sup><sub>p</sub>(quanta/cm<sup>2</sup>/sec)</b>			

The absorbed photo numbers in each semiconductor was calculated by the following equation:

$$R_p^a = \int_{400}^{800} S \times \alpha \times I$$

Where  $S = 0.19 \text{ cm}^2$  is the area of the electrode,  $\alpha$  is the light absorption and  $I$  is the light intensity at each wavelength.<sup>1</sup>

**Table S3.** Comparison of analytical parameters for chlorpyrifos detection in literatures.

<b>Method</b>	<b>Detection limit ( ng mL<sup>-1</sup>)</b>	<b>Linear range (ng mL<sup>-1</sup>)</b>	<b>references</b>
<b>LC-tandem MS</b>	<b>0.5</b>	<b>0.5-100</b>	2
<b>Surface- enhance-Raman spectra</b>	<b>10</b>	<b>10-50</b>	3
<b>PEC</b>	<b>3.5</b>	<b>70-5600</b>	4
<b>PEC</b>	<b>0.03</b>	<b>0.1-50</b>	5
<b>PEC</b>	<b>0.02</b>	<b>0.05-80</b>	6
<b>PEC</b>	<b>0.03</b>	<b>0.01-80</b>	This work

**Table S4.** The relative standard deviation of three  $\beta$ -Bi<sub>2</sub>O<sub>3</sub>-/CNNs 2%-based photoelectrode

photoelectrode	First detection ( $\mu$ A)	Second detection ( $\mu$ A)	Third detection ( $\mu$ A)	Relative standard deviation (%)
$\beta$ -Bi <sub>2</sub> O <sub>3</sub> /CNNs 2%	-1.2	-1.17	-1.21	
$\beta$ -Bi <sub>2</sub> O <sub>3</sub> /CNNs 2%- 10ng mL <sup>-1</sup> chlorpyrifos	-0.39	-0.303	-0.366	5.56

**Table S5.** Determination results of Chlopyrifos in real sample by the PEC method (n = 3).

sample	Added(ng mL <sup>-1</sup> )	Detected(ng mL <sup>-1</sup> )	Recovery(%)	Relative standard deviation (%)
1	0.05	0.052	104	1.04
2	0.2	0.2	100	1.4
3	1	1.09	109	4.9
4	10	9.8	98	4.4
5	20	20.4	102	5.1

1. M. Liu, X. Qiu, M. Miyauchi and K. Hashimoto, Energy-level matching of Fe(III) ions grafted at surface and doped in bulk for efficient visible-light photocatalysts, *J Am Chem Soc*, 2013, **135**, 10064-10072.
2. **P. 47 Salm**, P. J. Taylor, D. Roberts and J. de Silva, Liquid chromatography–tandem mass spectrometry method for the simultaneous quantitative determination of the



organophosphorus pesticides dimethoate, fenthion, diazinon and chlorpyrifos in human blood, *Journal of Chromatography B*, 2009, **877**, 568-574.

3. **J. 48 Tang**, W. Chen and H. Ju, Rapid detection of pesticide residues using a silver nanoparticles coated glass bead as nonplanar substrate for SERS sensing, *Sensors and Actuators B: Chemical*, 2019, **287**, 576-583.
4. **H. 49 Li**, J. Li, Q. Xu and X. Hu, Poly(3-hexylthiophene)/TiO<sub>2</sub> nanoparticle-functionalized electrodes for visible light and low potential photoelectrochemical sensing of organophosphorus pesticide chlorpyrifos, *Anal Chem*, 2011, **83**, 9681-9686.
5. **Q. 41 Liu**, Y. Yin, N. Hao, J. Qian, L. Li, T. You, H. Mao and K. Wang, Nitrogen functionalized graphene quantum dots/3D bismuth oxyiodine hybrid hollow microspheres as remarkable photoelectrode for photoelectrochemical sensing of chlorpyrifos, *Sensors and Actuators B: Chemical*, 2018, **260**, 1034-1042.
6. J. Qian, Z. Yang, C. Wang, K. Wang, Q. Liu, D. Jiang, Y. Yan and K. Wang, One-pot synthesis of BiPO<sub>4</sub> functionalized reduced graphene oxide with enhanced photoelectrochemical performance for selective and sensitive detection of chlorpyrifos, *Journal of Materials Chemistry A*, 2015, **3**, 13671-13678.